Matter and Radiation at Extremes

RESEARCH ARTICLE

pubs.aip.org/aip/mre

# Quantum splitting of electron peaks in ultra-strong fields

Cite as: Matter Radiat. Extremes 8, 054003 (2023); doi: 10.1063/5.0157663
Submitted: 9 May 2023 • Accepted: 30 July 2023 •
Published Online: 6 September 2023



Bo Zhang,[a] Zhi-Meng Zhang, and Wei-Min Zhou[b]

## AFFILIATIONS

Key Laboratory of Plasma Physics, Research Center of Laser Fusion, CAEP, Mianshan Rd 64, 621900 Mianyang, Sichuan, China

[a]Author to whom correspondence should be addressed: zhangbolfrc@caep.cn
[b]Electronic mail: zhouwm@caep.cn

## ABSTRACT

Effects of multiple nonlinear Compton scattering on electrons in ultra-strong fields are described using analytic formulas similar to those in the theory of multiple bremsstrahlung. Based on these analytic formulas, a new pure quantum effect of multiple nonlinear Compton scattering called quantum peak splitting is identified: the electron peak splits into two when the average number of nonlinear Compton scatterings per electron passes a threshold of 5.1 and is below 9. Quantum peak splitting stems from the discreteness of quantum radiation reaction, with one of the split peaks being formed by electrons emitting zero to three times and the other by electrons emitting four or more times. This effect provides a new mechanism for the formation of electron peaks, imposes a new beamstrahlung limit on future colliders, and corrects the picture of quantum radiation reaction. Experiments can be performed on lasers with intensities $\gtrsim 10^{21}$ W/cm$^2$, which are reachable on PW-scale facilities.



## I. INTRODUCTION

Nonlinear Compton scattering (NCS) is the scattering of an electron with coherent photons, i.e., $e + n\gamma_L \to e + \gamma$. It is a strong-field quantum electrodynamic (SFQED) process and is expected to be one of the dominant processes in ultra-high-intensity laser (UIL) fields. With recent progress in laser technology,[1–15] SFQED processes[16–31] have attracted wide research interest. The availability of 1–10 PW facilities[15] and new designs of high-energy colliders[32–35] have also encouraged investigations into new effects of NCS, such as interference effects,[36] nonperturbative SFQED,[37] quantum quenching,[38] peak broadening,[39] and electron trapping.[40,41]

The analytic theory of single NCS was established long ago.[42–44] However, NCS is a high-probability quantum process, and electrons usually emit multiple times in UIL pulses, and therefore most investigations of NCS so far have relied on numerical simulations or numerical solution of integral equations,[45] which are comparatively time-consuming and expensive tasks.

Peaks in spectra of particle beams are basic features. They are taken as strong evidence for new acceleration mechanisms in experiments and simulations[46–53] or possible clues for dark matter annihilation and decay.[54] An important constraint on high-energy colliders is that the radiation loss of the colliding beams at the interaction point should be within 20%.[32–35] Searching for peaks in the invariant mass spectrum is one of the main approaches for finding new particles, and the spectrum of invariant mass recoiling against observable particles has the prominent advantage of being independent of specific decay modes in the detection of Higgs bosons and the search for dark matter particles.[55–58]

In this work, analytic formulas for the effects of multiple NCS that are similar to the formulas in the theory of multiple bremsstrahlung are developed. Based on these formulas, a new pure quantum effect on electron dynamics in strong fields called quantum peak splitting is identified: when electrons propagate in ultra-strong fields and the average radiation per electron is ~5.1–9, the electron peak splits into two. This finding has a direct impact on electron dynamics in strong fields. It unveils a new stage of quantum radiation reaction and puts new constraints on future colliders. This new effect should also be important for the analysis of particle acceleration, and the detection of new particles, dark matter, and Higgs bosons, since the it can create fake peaks.

## II. APPROXIMATE BEHAVIOR OF SINGLE NCS AND SINGLE QSR

In ultra-strong fields, electron dynamics is mainly influenced by quantum emission of radiation and the reaction back on itself.

NCS and quantum synchrotron radiation (QSR) are very important radiation processes. NCS is the dominant process[16–23] and the major form of electron radiation when laser intensities reach levels of $\gtrsim 10^{21-23}$ W/cm$^2$ or higher, which are already achievable today.[1,15] QSR of electrons and positrons in the strong fields generated by opposite bunches at the interaction points of colliders[59–62] is called beamstrahlung.[32–35,63]

NCS and QSR have short coherence intervals in ultra-strong fields and are therefore usually taken as instantaneous and local processes, i.e., the local constant field approximation (LCFA) is adopted. $\chi \equiv e\sqrt{-(F_{\mu\nu}p^\nu)^2}/m^3$ is the key parameter of NCS and QSR,[16–20,64] where $F^{\mu\nu}$ is the electromagnetic field, $p^\nu$ is the electron four-momentum, $e$ is the electron charge, and $m$ is the electron mass. The differential probability of single NCS[42–44] is

$$\frac{dW_{\rm NCS}}{d\delta\, dt} = \frac{\alpha}{\pi\sqrt{3}}\frac{m^2}{p_0}\left[\left(1-\delta+\frac{1}{1-\delta}\right)K_{2/3}\left(\frac{2\delta}{3\chi(1-\delta)}\right) - \int_{2\delta/3\chi(1-\delta)}^{\infty} dy\, K_{1/3}(y)\right], \qquad \delta \in (0,1), \tag{1}$$

and that of single QSR is[64]

$$\frac{dW_{QSR}}{dt\, d\delta} = \frac{\sqrt{3}\alpha}{2\pi}\frac{m_q\chi_q}{\gamma}\frac{1-\delta}{\delta} \times\left[\kappa(y)+y^3\left(\frac{3\chi_q}{2}\right)^2(1-\delta)K_{2/3}(y)\right], \tag{2}$$

where $\alpha$ is the fine structure constant, $m_q$ and $\gamma$ are the mass and Lorentz factor of the charge, $\chi_q = \gamma B/B_q$ is the $\chi$ parameter in a pure magnetic field, $B$ is the magnetic field, and $B_q = m_q^2/q$ is the critical magnetic field. $\delta = k'k/pk$ for NCS and $\delta = k_0'/p_0$ for QSR. $p_0$ is the electron energy before radiation, and $k_0'$ is the emitted photon energy. For NCS of ultra-relativistic electrons, $\chi \approx \gamma(1-\cos\theta)a_0k_0/m$, where $\theta$ is the angle between electron and laser, $a_0 \equiv eE_L/m\omega_0$ is the normalized laser amplitude, and $E_L$ and $\omega_0$ are the laser electric field and frequency. The function $\kappa(y)$ is given by

$$\kappa(y) = y\int_y^{\infty} K_{5/3}(x)dx, \tag{3}$$

where $K_\nu(x)$ is the modified Bessel function of the $\nu$th order and

$$y = \frac{2\delta}{3\chi_q(1-\delta)}. \tag{4}$$

The differential probabilities of both NCS[42–44] and QSR[64–66] scale approximately as

$$\frac{dW}{d\delta\, dt} \propto \delta^{-2/3}e^{-\delta/\delta_0} \tag{5}$$

when $\delta \ll 1$ and $\chi$ or $\chi_q \ll 1$,[44,64] where $\delta = k_0'/p_0$ is the radiation loss rate and $\delta_0 \approx \chi$ or $\chi_q$ when $\chi$ or $\chi_q \ll 1$.

We use an interpolation function

$$f_{\rm in}(\delta) \approx A\frac{\alpha m^2}{p_0}\left(\frac{\chi}{\delta}\right)^{2/3}\exp\left(-\frac{\delta}{\chi}\right) \tag{6}$$

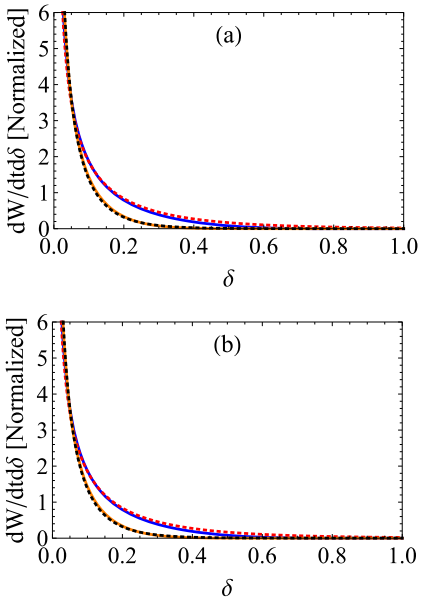


**FIG. 1.** (a) Comparison of normalized differential radiation probability of NCS (orange/blue solid curves for $\chi = 0.1/0.3$) with the approximation (black/red dotted curves for $\chi = 0.1/0.3$). (b) Comparison of normalized differential radiation probability of QSR (orange/blue solid curves for $\chi = 0.1/0.3$) with the approximation (black/red dotted curves for $\chi = 0.1/0.3$).

to test this approximation. The comparisons in Fig. 1 show that this approximation agrees well with Eqs. (1) and (2) in the region where $\delta \ll 1$ and $\chi \ll 1$. Note that this region covers the main part of $f_{\rm in}$ and the parameter space that existing and near-future experiments can reach ($\chi \lesssim 0.3$). The unphysical part of this approximation is less than 0.6% $\left[\int_1^{\infty} f_{\rm in}(x)dx/\int_0^{\infty} f_{\rm in}(x)dx\right]$ when $\chi \lesssim 0.3$.

## III. ANALYTIC THEORY FOR MULTIPLE NCS AND MULTIPLE QSR

We will restrict our discussion of multiple NCS to the weak radiation-dominated regime (WRDR), where $\chi \ll 1$ and $a_0 \ll \chi\gamma$. The former ensures that most emissions only consume a small fraction of the electron energy and the latter ensures that the influence of the Lorentz force on electrons is much weaker compared with that of radiation. The WRDR is important because experiments on NCS so far[67,68] and the beamstrahlung of existing colliders fall in this regime. In the WRDR, pair production is suppressed, electrons lose only a small fraction of energy through most emissions, and the influence of the electromagnetic force is much weaker than that of NCS, and hence electron dynamics is dominated by weak emissions that can be treated as perturbations.

We will show that the effects of multiple NCS and QSR in the WRDR can be described analytically. Consider a physical quantity $x$ (spin, energy, angle, etc.) of an electron beam propagating in ultra-strong fields in the WRDR. The distribution function $F(x)$ normalized by electron number is approximately

$$F(x) = P_0f_0(x) + \sum_{i=1}^{\infty} P_if_i(x), \tag{7}$$

where $P_i$ is the probability of emitting $i$ times ($\sum P_i = 1$) and $f_i$ are the normalized spectra of electrons radiating $i$ times ($\int f_i(x)dx = 1$).

$P_i$ has an analytic approximation, which is possible because the emission rate in the WRDR is almost unmodified by quantum emissions. The radiation rate of NCS,

$$\frac{dW_{\rm NCS}}{dt} = \int_0^1 d\delta \frac{dW}{d\delta\, dt} \approx \frac{1.44\alpha\chi m}{\gamma\hbar} \approx 0.01(1-\cos\theta)a_0\omega_0, \quad (8)$$

is approximately proportional to $a_0$[38,44] and approximately independent of $\gamma$ in the WRDR, where $r$ is the average number of emissions per electron. Similarly, in the WRDR, the emission rate of QSR,[64–66]

$$\frac{dW_{QSR}}{dt} \approx \frac{5\alpha Bm}{2\sqrt{3}B_q\hbar}, \quad (9)$$

is also approximately proportional to the external field and insensitive to $\gamma$.[61] Since there is almost no modification of the emission rate by NCS and QSR, $P_i$ is approximately determined by the fields. According to probability theory,[71] the number of emissions $i$ approximately follows a Poisson distribution, i.e.,

$$P_i(r) \approx \frac{r^i}{i!}e^{-r} \quad (i \geq 0). \quad (10)$$

This is similar to the distribution of multiple bremsstrahlung.[69,70] As shown in Fig. 2(a), this simple approximation agrees very well with the simulation results. The distribution peaks at $i = [r]$, where $[r]$ denotes the integer part of $r$, and the width of the distribution is of the scale of $\sqrt{r}$.

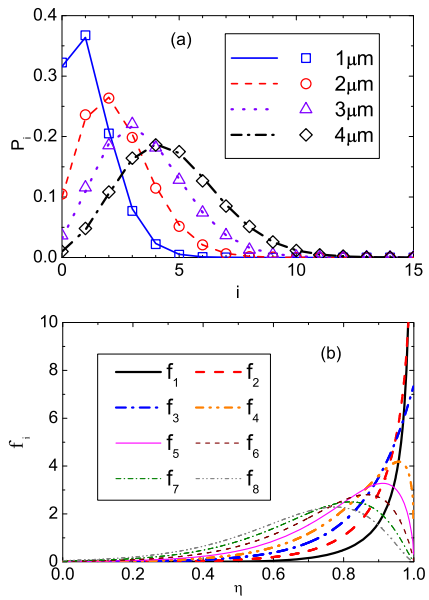


**FIG. 2.** (a) Comparison of $P_i$ distributions given by simulations (symbols) and their analytic approximations (curves) of $p_0 = 1.5$ GeV electrons propagating 1–4 $\mu$m ($r = 1.15, 2.3, 3.45$, and 4.6) perpendicularly in a $\lambda_0 = 800$ nm, circularly polarized laser with $I = 1 \times 10^{21}$ W/cm$^2$. (b) Functions $f_i$.

We develop an analytic approximation for $f_i(x)$ in the comparatively simple case that $x$ is the electron energy. In the WRDR, radiation reaction can be taken as a perturbation to the electron energy, and hence

$$f_i(\eta) \approx \int d\eta' f_{i-1}(\eta')\bar{R}(\eta'-\eta) \quad (i \geq 1), \quad (11)$$

where $\eta = E/E_0$ is the electron energy $E$ normalized by the primary energy $E_0$, and

$$\bar{R}(\delta) = \frac{\int dt \frac{dW}{d\delta\, dt}}{\int d\delta \int dt \frac{dW}{d\delta\, dt}} \quad (12)$$

is the normalized average differential radiation probability for a electron with $p_0 = E_0$ to emit a photon with $k_0 = \delta E_0$.

In the simplest case of a constant external field, since the most emissions fall in the $\delta \ll 1$ region and $R(\delta)$ is approximately proportional to $\delta^{-2/3}e^{-\delta/\chi}$ in the WRDR,

$$R(\delta) \approx R^A(\delta) = \frac{\chi^{-1/3}\delta^{-2/3}}{\Gamma(1/3)}e^{-\delta/\chi}. \quad (13)$$

Then, for a quasi-monoenergetic electron beam, according to Eq. (11), an analytic approximation

$$f_{i,\chi}(\eta) \approx f^A_{i,\chi}(\eta) = \frac{\chi^{-i/3}}{\Gamma(i/3)}(1-\eta)^{i/3-1}e^{-(1-\eta)/\chi} \quad (14)$$

for $i \geq 1$ is obtained, which is similar to the expression in the case of multiple bremsstrahlung[69,70] if screening effects are significant. This analytic approximation $f_i^A$ shows that $f_i$ increases monotonically and peaks at $\eta = 1$ when $i = 1, 2, 3$. When $i \geq 4$, $f_i^A$ vanishes at $\eta = 1$ and $\eta = 0$ and peaks at $\eta = 1 - (\chi/3)(i-3)$. The peak jumps with a step of $\Delta\eta = \chi/3$ as $i$ increases. These features predicted by $f_i^A$ are confirmed by the functions $f_i(\eta)$ obtained by numerical integration of Eq. (11) and shown in Fig. 2(b). The unphysical part of $f_i(\eta < 0)$ obtained with Eq. (11) is within 0.5% when $\chi < 0.10$ and $i \leq 10$, and the unphysical part of $F(\eta)$ is less than 1% when $r < 10$ and $\chi < 0.10$.

## IV. TEST OF THE ANALYTIC FORMULAS

In Sec III, we developed analytic formulas for the electron spectrum after stochastic emissions of radiation in the WRDR. The analytic approximation is very simple when the electron bunch has a narrow primary energy divergence.

We compare the results of the analytic formulas for multiple NCS with those of Monte Carlo simulations. We employed the program used in Refs. 72 and 73 to carry out the simulations. In these simulations, emissions of radiation were included as instantaneous and local processes. Between emissions, the classical equations of motion described the laser Lorentz force and particle propagation. The laser fields of the tightly focused laser used in the simulations were those given in Ref. 74. The 0.8 $\mu$m laser lasted for $\tau_0 = 2\lambda/c = 30$ fs, its peak intensity was $I_0 = 2.74(a_0/\lambda_0[\mu\text{m}])^2 \times 10^{18}$ W/cm$^2$ $= 5 \times 10^{20}$ W/cm$^2$, and the laser waist was 3.6 $\mu$m. $N = 10^5$ electrons were primarily distributed uniformly in a $D = 0.8$ $\mu$m sphere. The electron beam and the laser pulse were

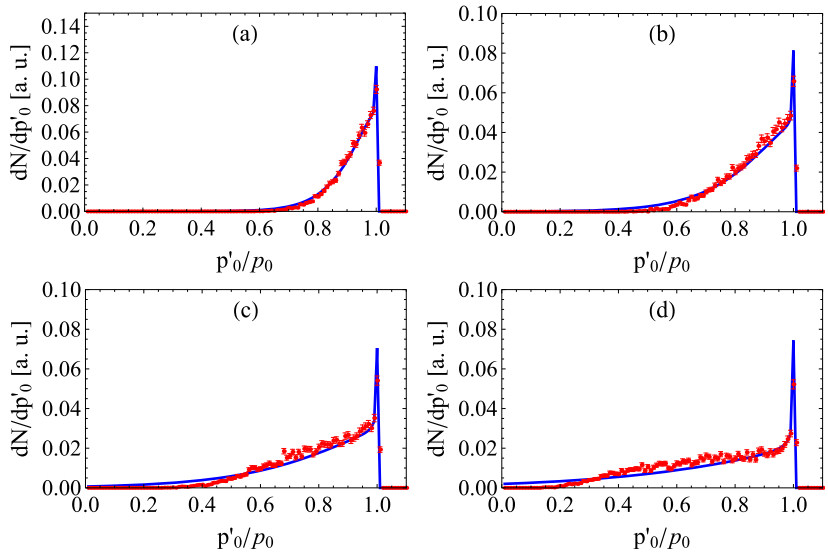


**FIG. 3.** Comparison of the analytic formulas (curves) and simulations (symbols) for the electron spectrum after multiple NCS. Electrons with $p_0$ = 0.5 GeV (a), 1.0 GeV (b), 2.0 GeV (c), and 5.0 GeV (d) propagate perpendicularly through the waist of a $\lambda$ = 800 nm circularly polarized laser that lasts for $\tau$ = 30 fs. The peak laser intensity is $5 \times 10^{20}$ W/cm$^2$ and the laser waist is 3.6 $\mu$m. $\chi_0 = a_0 p_0 k_0/m^2$ is 0.05, 0.1, 0.2 and 0.5, respectively, in (a)–(d).

perpendicular to each other, and they were both 15 $\mu$m from the focus before the simulations, which lasted for 100 fs, with a time step of $1.67 \times 10^{-2}$ fs. The electromagnetic force between the electrons was ignored, since the it was four to five orders of magnitude weaker than the laser Lorentz force. Pair production was ignored, since the its probability is strongly suppressed when $\chi < 1$.[67,68] Other SFQED effects and processes[24–31] are also negligible in the WRDR, owing to their low probabilities; a detailed method to estimate the significance of other SFQED processes can be found in the supplementary information of Ref. 73. Figures 3(a)–3(c) show that the analytic formula agrees well with the simulations when $\chi_0 \ll 1$. Even in the $\chi_0 = 0.5$ case [Fig. 3(d)], the agreement is not bad.

## V. QUANTUM PEAK SPLITTING

With the analytic approximations of $P_i$ and $f_i$ in Eqs. (10) and (14), we can give a complete picture of the electron spectrum deformation caused by quantum radiation reaction induced by NCS and QSR in the WRDR. When $r$ is small, most electrons only emit a few times, $f_0$ to $f_3$ dominate the spectrum, and the spectral peak stays at $\eta = 1$, as shown by the simulation results in Fig. 4(a). We employed the programs used in Refs. 72 and 73 to carry out the simulations. In these simulations, NCS and pair production were included, although the latter is negligible because the probability of pair production is strongly suppressed in $\chi < 1$ regions.[67,68] The classical equations of motion described the laser Lorentz force and electron propagation between emissions. The electromagnetic forces between the charges were four to five orders of magnitude weaker than the laser Lorentz force, and therefore were also ignored. Note that $i = 0$ electrons, i.e., quantum quenching of radiation, were believed to suspend the peak shift,[38] but actually all the electrons radiating $i = 0, \ldots, 3$ times contribute.

When $r$ has moderate values, both $i = 0, \ldots, 3$ and $i \geq 4$ electrons are important. The functions $f_{i\geq 4}$ strongly overlap with each other, and hence the $i \geq 4$ electrons together form a peak, i.e., the spectral peak splits into two, as shown in Fig. 4(b). With further increase in $r$, the contributions of $i \leq 3$ electrons and thus also the peak at $\eta = 1$ decay rapidly and eventually disappear when $r \sim 9$, as shown in Fig. 4(c).

A complete peak splitting process is shown in Fig. 4(d), and the contributions from $i \leq 3$ and $i \geq 4$ electrons are shown separately in Figs. 4(e) and 4(f). These results clearly confirm the composition of the two split peaks: one is formed by electrons emitting zero to three times and the other by electrons emitting ≥4 times, and the origin of the quantum peak splitting is the discreteness of NCS/QSR.

The normalized spectra of emitted photons when the electron beam has propagated $D$ = 1, 2, and 4 $\mu$m shown in Figs. 4(a)–4(c) are almost the same. This verifies the assumption we adopted to obtain the analytic formulas (10)–(14), namely, that the differential radiation probability of successive NCS is insensitive to NCS emissions in the WRDR.

This new picture of electron dynamics in strong fields corrects the conventional picture and makes it self-consistent. The conventional picture is based on two longstanding, widely accepted, but incompatible concepts about electron dynamics in strong fields. On the one hand, since the radiation decreases the electron energy, it naturally can shift the electron peak. On the other hand, quantum quenching of radiation loss can lock the electron peak at the primary energy.[32,33,38] So, the conventional diagram shown in Fig. 5(a) needs a transition point. However, a peak locked by quantum quenching of radiation loss cannot shift anyway, and therefore such a transition point cannot exist. With quantum peak splitting, a new stage

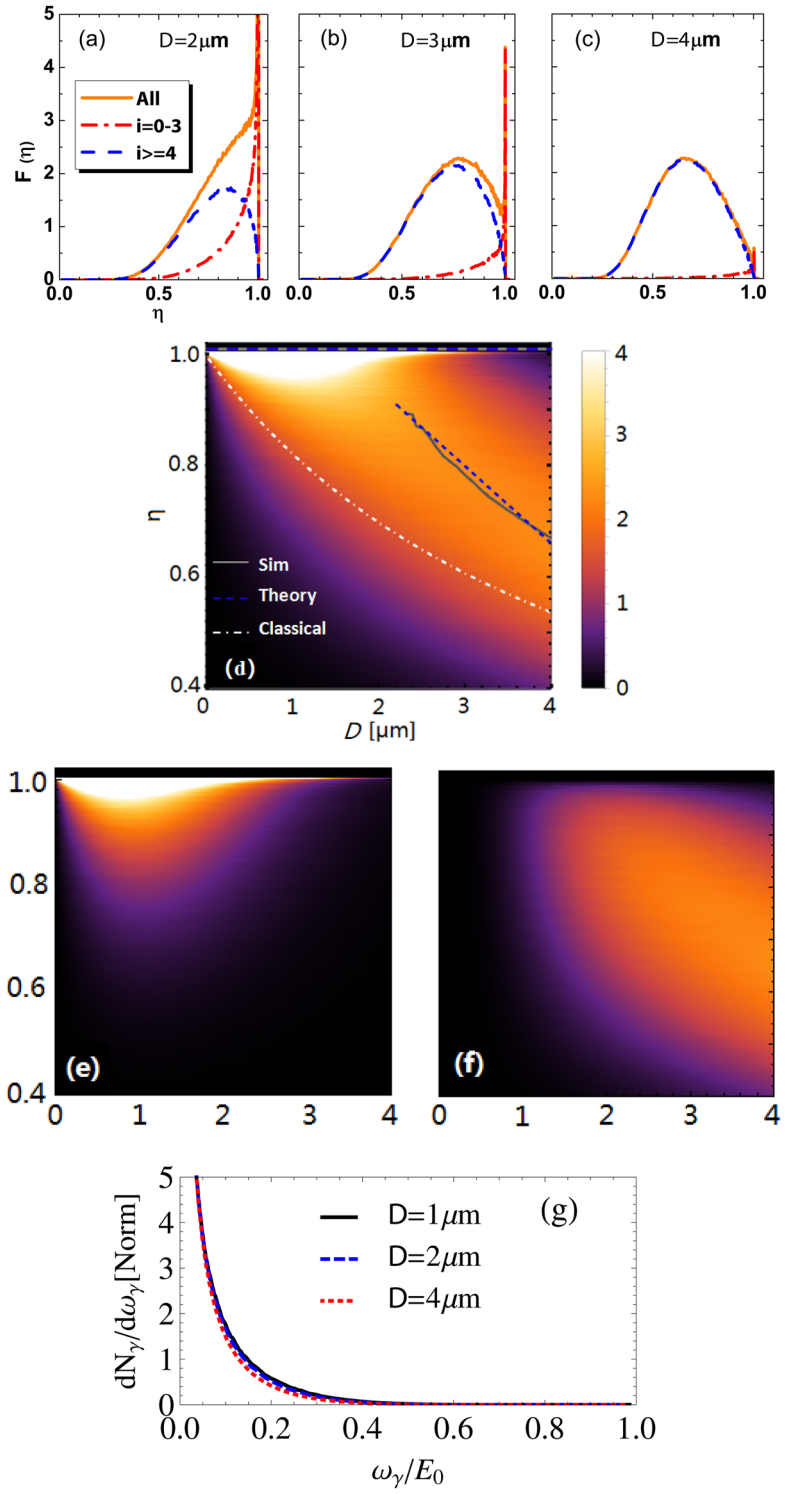


**FIG. 4.** Peak splitting process. (a), (b), and (c) Spectra of a 1 GeV electron beam after it has propagated respectively $D = 2, 3$, and 4 $\mu$m perpendicularly in a $\lambda = 800$ nm circularly polarized laser with $I = 4 \times 10^{21}$ W/cm$^2$, corresponding respectively to $r = 4.6, 6.9$, and 9.2. (d), (e), and (f) Spectra for respectively all electrons, $i \leq 3$ electrons, and $i \geq 4$ electrons in the whole peak splitting process. The curves in (d) show the peaks given by classical theory (white dot-dashed), analytic quantum theory (blue dashed), and simulation (gray solid). (g) Normalized spectra of emitted $\gamma$ rays after the electron beam has propagated different distances.

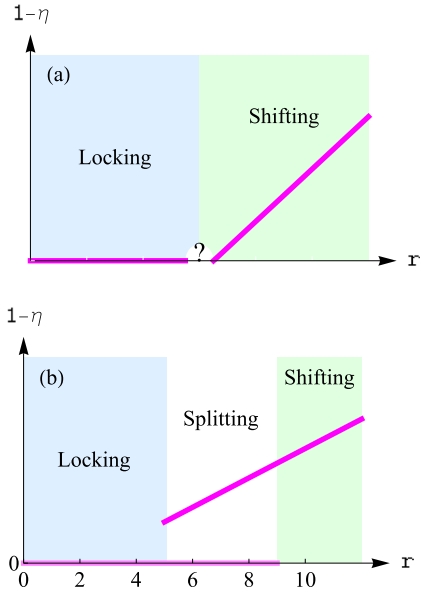


**FIG. 5.** Sketches of (a) conventional and (b) new diagrams for quantum radiation reaction stages. The purple lines are peaks of the electron spectrum, $r$ is the average number of emissions, and $\eta$ is the energy normalized by the primary energy.

is inserted between the peak locking and shifting stages, as shown in Fig. 5(b), and the picture of electron dynamics in strong fields becomes self-consistent.

Such peak splitting is a pure quantum effect induced by the discreteness of quantum emissions of radiation. In classical theory,[75,76] continuous and deterministic radiation reaction shifts the peak continuously and nonlinearly rather than splitting it, as shown in Fig. 4(d).

A feature of quantum peak splitting is that the derivative of the spectrum,

$$\partial_\eta F(\eta) \approx -\chi \sum_{i=1}^{\infty} \frac{r^i[(i/3-1)\xi^{i/3-2} - \xi^{i/3-1}]}{i!\Gamma(i/3)} e^{-r} e^{-\xi}, \tag{15}$$

has a zero point between $\eta = 0$ and $\eta = 1$, where $\xi = (1-\eta)/\chi$. Since the this is a series in $\eta$ whose coefficients are determined by $r$, the threshold for quantum peak splitting is determined by the value of $r$. We obtain $r = 5.35$ by solving the equation numerically. In our simulations, the splitting of the peak is slightly earlier: it usually happens around $r = 5.1$. Hence, the average number of emissions $r$ controls the quantum peak splitting process.

Then what is the interval between split peaks? The $P_i$ distribution is approximately symmetric around $i = [r]$ when $r$ is near $[r] + 1/2$. Hence, the peak formed by $i \geq 4$ electrons is located near $\eta = 1 - (\chi/3)(r - 3.5)$, and the interval between the split peaks is

$$\Delta\eta_{\text{peak}} \approx \frac{\chi}{3}(r - 3.5). \tag{16}$$

The splitting interval is compared with simulations in Fig. 4(d): it grows linearly with $r$ as long as $\Delta\eta_{\text{peak}}$ is not too large, i.e., ≤0.5. The initial position of the $i \geq 4$ peak when it splits from the $i = 0, \ldots, 3$ peak is then at $\eta \approx 1 - \chi/2$. An additional condition for quantum peak splitting is that this splitting should not be flooded by the primary beam energy spread $\Delta\eta_0$, i.e., $\Delta\eta_0 < \Delta\eta_{\text{peak}}$.

## VI. QUANTUM PEAK SPLITTING IN BEAM–BEAM INTERACTIONS

In colliders, quantum radiation reaction can also split the peaks of the luminosity spectrum, i.e., the center-of-mass energy distribution at the interaction point, and this is due to quantum beamstrahlung. In most future $e^+e^-$ collider designs, the two bunches are symmetric, and the beamstrahlung parameter $\chi_{e^-} = \chi_{e^+} = \chi$. When $\chi \ll 1$, the beamstrahlung energy loss $\Delta E$ is small compared with the primary energy $E_0$, and then $\eta_{\text{cm}} \equiv \sqrt{s}/2E_0 \approx 1 - (\Delta E_{e^-} + \Delta E_{e^+})/2E_0$. In this case, the luminosity spectrum

$$F(\eta_{\text{cm}}) \approx \sum_{i,i'=0}^{\infty} P_i(n_{\gamma,e^-}) P_{i'}(n_{\gamma,e^+}) \times \int_{\eta_{\text{cm}}}^{1} d\eta'_{\text{cm}}\, f^A_{i,\chi/2}(\eta'_{\text{cm}}) f^A_{i',\chi/2}(1 - \eta'_{\text{cm}} + \eta_{\text{cm}}), \tag{17}$$

where $n_{\gamma,e^-/e^+}$ is the average emission number of an $e^-/e^+$ bunch. Considering

$$f^A_{i,\chi}(\eta) \approx \int_{\eta}^{1} d\eta'\, f^A_{i',\chi}(\eta) f^A_{i-i',\chi}(1 + \eta - \eta') \tag{18}$$

and

$$P_k(n_{\gamma,e^-} + n_{\gamma,e^+}) = \sum_{k'=0}^{k} P_{k'}(n_{\gamma,e^-}) P_{k-k'}(n_{\gamma,e^+}), \tag{19}$$

the luminosity spectrum has a simple approximation

$$F(\eta_{\text{cm}}) \approx \sum_{k=0}^{\infty} P_k(2n_\gamma) f^A_{i,\chi/2}(\eta_{\text{cm}}). \tag{20}$$

Hence, when $n_{\gamma,e^-} + n_{\gamma,e^+}$ fall between 5.1 and 9, i.e., $n_\gamma = n_{\gamma,e^-} = n_{\gamma,e^+}$ fall between 2.55 and 4.5, the peak in the luminosity spectrum will split.

If this happened in a collider, its application and performance would be limited by such a double-peaked structure of the luminosity spectrum. This is especially severe for experiments based on measurements of invariant mass recoiling against observable particles,[55–58] which have the prominent advantage of being independent of specific decay modes when probing particles that are hard to detect directly in processes such as Higgstrahlung $e^+e^- \to Zh \to \mu^+\mu^- h$ and processes producing dark matter $e^+e^- \to \tilde{D}D + X$, where $X$ can be a $\gamma$, a photon, a single jet, a $Z$ boson, etc. In these experiments, peaks in the spectrum of invariant mass recoiling against observable particles are the main signals, and thus split peaks in the luminosity spectrum may introduce fake signals.

The conventional constraint on beamstrahlung in colliders is that the average energy loss should be within 10%–20%. Since the average energy loss per emission has an upper limit ~25% even in $\chi \gg 1$ regions, this constraint is also usually expressed as the requirement that $n_\gamma$ should not go far beyond 1, i.e., $n_\gamma \lesssim 1$. With increasing

demands on energy and luminosity, $n_\gamma$ has increased rapidly, and has already reached 2.2[32–35] in collider designs. Quantum peak splitting brings in a new constraint of $n_\gamma < 2.55$.

Quantum peak splitting also provides a new mechanism for peak formation. New peaks are usually taken as strong evidence for new acceleration mechanisms[46–53] or the decay of unknown particles.[54] Quantum peak splitting provides a new possibility, especially in a strong-field background such as in ultra-strong laser experiments.

## VII. DISCUSSIONS AND CONCLUSION

The above investigations have been limited to the WRDR where $\chi \ll 1$. A natural question is whether quantum peak splitting occurs when $\chi \lesssim 1$ or $\gg 1$. Although a thorough understanding of this needs further careful research, we expect that quantum peak splitting will also exist in $\chi \lesssim 1$ regions. When $\chi \lesssim 1$, a large portion of electrons will lose a large ratio of their energies in a few emissions. Therefore, the split peaks will be located at $\eta = 1$ and $\eta \sim 0$, the threshold for quantum peak splitting will be different from $r = 5.1$, and therefore the distance between split peaks can no longer be described by Eq. (16). When $\chi \gg 1$, pair production will become significant, and therefore the analytic description of the electron spectrum needs to incorporate it.

In conclusion, inspired by the theory of multiple bremsstrahlung, analytic formulas to describe the effects of multiple NCS and QSR on the electron spectrum have been developed. Using these formulas, the electron spectrum deformations induced by quantum radiation reaction in the weak radiation-dominated regime have been investigated, and a new pure quantum effect of multiple NCS/QSR called quantum peak splitting has been found. Most electron beams produced by accelerators have a single peak in the spectrum, but after propagating in ultra-strong fields, this peak can split owing to the quantum nature of the emissions (NCS/QSR). Electrons that radiate $i = 0, \ldots, 3$ times form one peak, and electrons that radiate $i \geq 4$ times form the other. The condition for quantum peak splitting in the WRDR is that electrons radiate $r \sim 5.1$–$9$ times on average. As well as being a new phenomenon, quantum peak splitting also has an impact in three ways. First, newly formed peaks in charged particle spectra are usually attributed to particle acceleration or decay, and quantum peak splitting provides a third mechanism. Second, quantum peak splitting makes the picture of quantum radiation reaction self-consistent, since the it introduces a new splitting stage. Third, quantum peak splitting imposes a new constraint on future colliders that the electrons/positrons should radiate less than 2.55 times on average, otherwise the luminosity spectrum would have two peaks.

## ACKNOWLEDGMENTS

The authors would like to thank Bin Zhu, Dr. Gang Li, and Dr. Professor Wei Hong for fruitful discussions. This work is supported by the National Key Program for Science and Technology Research and Development (Grant No. 2018YFA0404804), the Science and Technology on Plasma Physics Laboratory, Laser Fusion Research Center Funds for Young Talents (Grant No. RCFPD2-2018-4), and the National Natural Science Foundation of China (Grant No. 11805181).

## AUTHOR DECLARATIONS

### Conflict of Interest

The authors have no conflicts to disclose.

### Author Contributions

**Bo Zhang**: Conceptualization (equal); Funding acquisition (equal); Investigation (equal); Software (equal); Writing – original draft (equal); Writing – review & editing (equal). **Zhi-Meng Zhang**: Funding acquisition (equal); Investigation (equal); Software (equal); Writing – review & editing (equal). **Wei-Min Zhou**: Conceptualization (equal); Funding acquisition (equal); Writing – original draft (equal); Writing – review & editing (equal).

## DATA AVAILABILITY

The data that support the findings of this study are available from the corresponding author upon reasonable request.

## REFERENCES

[1] J. W. Yoon *et al.*, "Realization of laser intensity over $10^{23}$ W/cm$^2$," Optica **8**, 630 (2021).
[2] S. Weber *et al.*, "P3: An installation for high-energy density plasma physics and ultra-high intensity laser–matter interaction at ELI-beamlines," Matter Radiat. Extremes **2**, 149 (2017).
[3] C. Danson *et al.*, "Vulcan Petawatt—An ultra-high-intensity interaction facility," Nucl. Fusion **44**, S239 (2004).
[4] Exawatt Center for Extreme Light Studies (XCELS), http://www.xcels.iapras.ru/.
[5] Z. Guo *et al.*, "Improvement of the focusing ability by double deformable mirrors for 10-PW-level Ti: Sapphire chirped pulse amplification laser system," Opt. Express **26**, 26776 (2018).
[6] J. Zou *et al.*, "Design and current progress of the Apollon 10 PW project," High Power Laser Sci. Eng. **3**, e2 (2015).
[7] S. Gales *et al.*, "The extreme light infrastructure—Nuclear physics (ELI-NP) facility: New horizons in physics with 10 PW ultra-intense lasers and 20 MeV brilliant gamma beams," Rep. Prog. Phys. **81**, 094301 (2018).
[8] J. Bromage *et al.*, "Technology development for ultraintense all-OPCPA systems," High Power Laser Sci. Eng. **7**, e4 (2019).
[9] E. Cartlidge, "The light fantastic," Science **359**, 382 (2018).
[10] G. Tiwari *et al.*, "Beam distortion effects upon focusing an ultrashort petawatt laser pulse to greater than $10^{22}$ W/cm$^2$," Opt. Lett. **44**, 2764 (2019).
[11] X. Zeng *et al.*, "Multi-petawatt laser facility fully based on optical parametric chirped-pulse amplification," Opt. Lett. **42**, 2014–2017 (2017).
[12] V. Yanovsky *et al.*, "Ultra-high intensity-300-TW laser at 0.1 Hz repetition rate," Opt. Express **16**, 2109–2114 (2008).
[13] A. S. Pirozhkov *et al.*, "Approaching the diffraction-limited, bandwidth-limited petawatt," Opt. Express **25**, 20486 (2017).
[14] J. W. Yoon *et al.*, "Achieving the laser intensity of $5.5 \times 10^{22}$ W/cm$^2$ with a wavefront-corrected multi-PW laser," Opt. Express **27**, 20412 (2019).
[15] C. N. Danson *et al.*, "Petawatt and exawatt class lasers worldwide," High Power Laser Sci. Eng. **7**, e54 (2019).
[16] M. Marklund and P. K. Shukla, "Nonlinear collective effects in photon–photon and photon–plasma interactions," Rev. Mod. Phys. **78**, 591–640 (2006).
[17] F. Ehlotzky, K. Krajewska, and J. Z. Kamiński, "Fundamental processes of quantum electrodynamics in laser fields of relativistic power," Rep. Prog. Phys. **72**, 046401 (2009).

[18] A. Di Piazza, C. Müller, K. Z. Hatsagortsyan, and C. H. Keitel, "Extremely high-intensity laser interactions with fundamental quantum systems," Rev. Mod. Phys. **84**, 1177–1228 (2012).
[19] G. Mourou and T. Tajima, "Summary of the IZEST science and aspiration," Eur. Phys. J. Spec. Top. **223**, 979 (2014).
[20] A. Di Piazza *et al.*, Extreme Light Infrastructure: Report on the Grand Challenges Meeting, 2009.
[21] A. Gonoskov, T. G. Blackburn, M. Marklund, and S. S. Bulanov, "Charged particle motion and radiation in strong electromagnetic fields," Rev. Mod. Phys. **94**, 045001 (2022).
[22] P. Zhang, S. S. Bulanov, D. Seipt, A. V. Arefiev, and A. G. R. Thomas, "Relativistic plasma physics in supercritial fields," Phys. Plasmas **27**, 050601 (2020).
[23] A. Fedotov, A. Ilderton, F. Karbstein, B. King, D. Seipt, H. Taya, and G. Torgrimsson, "Advances in QED with intense background fields," Phys. Rep. **1010**, 1–138 (2023).
[24] J. Schwinger, "On gauge invariance and vacuum polarization," Phys. Rev. **82**, 664 (1951).
[25] J. Klein and B. Nigam, "Birefringence of the vacuum," Phys. Rev. **135**, B1279 (1964).
[26] S. L. Adler, J. N. Bahcall, C. G. Callan, and M. N. Rosenbluth, "Photon splitting in a strong magnetic field," Phys. Rev. Lett. **25**, 1061 (1970).
[27] W. G. Unruh, "Notes on black-hole evaporation," Phys. Rev. D **14**, 870 (1976).
[28] F. Mackenroth and A. Di Piazza, "Nonlinear double compton scattering in the ultrarelativistic quantum regime," Phys. Rev. Lett. **110**, 070402 (2013).
[29] B. King, A. Di Piazza, and C. H. Keitel, "A matterless double slit," Nat. Photonics **4**, 92 (2010).
[30] G. V. Dunne, H. Gies, and R. Schützhold, "Catalysis of Schwinger vacuum pair production," Phys. Rev. D **80**, 111301(R) (2009).
[31] B. Zhang *et al.*, "Vacuum radiation induced by time dependent electric field," Phys. Lett. B **767**, 431 (2017).
[32] C. Adolphsen *et al.*, "The international linear collider technical design report, volume III: Accelerator," arXiv:1306.6328 (2013).
[33] M. Aicheler, P. Burrows, M. Draper, T. Garvey, P. Lebrun, K. Peach, N. Phinney, H. Schmickler, D. Schulte, and N. Toge, A Multi-TeV Linear Collider Based on CLIC Technology: CLIC Concenptual Design Report. CERN-2012-007, 2012.
[34] The CEPC study group, "CEPC conceptual design report, volume I: Accelerator," arXiv:1809.00285 (2018).
[35] FCC collaboration, "FCC-ee: The lepton collider," Eur. Phys. J. Spec. Top. **228**, 261–623 (2019).
[36] V. Dinu, C. Harvey, A. Ilderton, and M. Marklund, "Quantum radiation reaction: From interference to incoherence," Phys. Rev. Lett. **116**, 044801 (2016).
[37] V. Yakimenko, S. Meuren, F. Del Gaudio, C. Baumann, A. Fedotov, F. Fiuza, T. Grismayer, M. J. Hogan, A. Pukhov, L. O. Silva, and G. White, "Prospect of studying nonperturbative QED with beam–beam collisions," Phys. Rev. Lett. **122**, 190404 (2019).
[38] C. N. Harvey, A. Gonoskov, A. Ilderton, and M. Marklund, "Quantum quenching of radiation losses in short laser pulses," Phys. Rev. Lett. **118**, 105004 (2017).
[39] N. Neitz and A. Di Piazza, "Stochasticity effects in quantum radiation reaction," Phys. Rev. Lett. **111**, 054802 (2013).
[40] L. L. Ji, A. Pukhov, I. Y. Kostyukov, B. F. Shen, and K. Akli, "Radiation–reaction trapping of electrons in extreme laser fields," Phys. Rev. Lett. **112**, 145003 (2014).
[41] A. Gonoskov, A. Bashinov, I. Gonoskov, C. Harvey, A. Ilderton, A. Kim, M. Marklund, G. Mourou, and A. Sergeev, "Anomalous radiative trapping in laser fields of extreme intensity," Phys. Rev. Lett. **113**, 014801 (2014).
[42] A. I. Nikishov and V. I. Ritus, "Quantum processes in the field of a plane electromagnetic wave and in a constant field," Zh. Eksp. Teor. Fiz. **46**, 776 (1964).
[43] A. I. Nikishov and V. I. Ritus, "Pair production by a photon and photon emission by an electron in the field of an intense electromagnetic wave and in a constant field," Zh. Eksp. Teor. Fiz. **53**, 1707 (1967).
[44] V. I. Ritus, "Quantum effects of the interaction of elementary particles with an intense electromagnetic field," J. Sov. Laser Res. **6**, 497 (1985).
[45] A. Di Piazza, K. Z. Hatsagortsyan, and C. H. Keitel, "Quantum radiation reaction effects in multiphoton compton scattering," Phys. Rev. Lett. **105**, 220403 (2010).
[46] H. Zhang, B. F. Shen, W. P. Wang, S. H. Zhai *et al.*, "Collisionless shock acceleration of high-flux quasimonoenergetic proton beams driven by circularly polarized laser pulses," Phys. Rev. Lett. **119**, 164801 (2017).
[47] F. Mackenroth *et al.*, "Chirped-standing-wave acceleration of ions with intense lasers," Phys. Rev. Lett. **117**, 104801 (2016).
[48] S. Palaniyappan *et al.*, "Efficient quasi-monoenergetic ion beams from laser-driven relativistic plasmas," Nat. Commun. **6**, 10170 (2015).
[49] J. H. Bin, W. J. Ma *et al.*, "Ion acceleration using relativistic pulse shaping in near-critical-density plasmas," Phys. Rev. Lett. **115**, 064801 (2015).
[50] X. F. Shen, A. Pukhov, and B. Qiao, "Monoenergetic high-energy ion source via femtosecond laser interacting with a microtape," Phys. Rev. X **11**, 041002 (2021).
[51] C. A. J. Palmer *et al.*, "Monoenergetic proton beams accelerated by a radiation pressure driven shock," Phys. Rev. Lett. **106**, 014801 (2011).
[52] C. Scullion *et al.*, "Polarization dependence of bulk ion acceleration from ultrathin foils irradiated by high-intensity ultrashort laser pulses," Phys. Rev. Lett. **119**, 054801 (2017).
[53] R. Matsui, Y. Fukuda, and Y. Kishimoto, "Quasimonoenergetic proton bunch acceleration driven by hemispherically converging collisionless shock in a hydrogen cluster coupled with relativistically induced transparency," Phys. Rev. Lett. **122**, 014804 (2019).
[54] G. Ambrosi *et al.* DAMPE collaboration, "Direct detection of a break in the teraelectronvolt cosmic-ray spectrum of electrons and positrons," Nature **552**, 63 (2017).
[55] H. Baer *et al.*, "The international linear collider technical design report, volume II: Physics," arXiv:1306.6352 (2013).
[56] L. Linssen, A. Miyamoto, M. Stanitzki, and H. Weerts, Physics and Detectors at CLIC: CLIC Conceptual Design Report. CERN-2012-003, 2012.
[57] The CEPC study group, "CEPC conceptual design report, volume II: Physics and detector," arXiv:1811.10545 (2018).
[58] A. Abada *et al.*, "FCC physics opportunities," Eur. Phys. J. C **79**, 474 (2019).
[59] K. K. Andersen *et al.* CERN (NA63), "Experimental investigations of synchrotron radiation at the onset of the quantum regime," Phys. Rev. D **86**, 072001 (2012).
[60] A. Bogomyagkov, E. Levichev, and D. Shatilov, "Beam–beam effects investigation and parameters optimization for a circular $e^+e^-$ collider at very high energies," Phys. Rev. Spec. Top.-Accel. Beams **17**, 041004 (2014).
[61] K. Yokoya and P. Chen, "Beam–beam phenomena in linear colliders," in Frontiers of Particle Beams: Intensity Limitations, Lecture Notes in Physics, edited by M. Dienes, M. Month, and S. Turner (Springer, Berlin, Heidelberg, 1992), Vol. 400.
[62] V. Shiltsev and F. Zimmermann, "Modern and future colliders," Rev. Mod. Phys. **93**, 015006 (2021).
[63] V. I. Telnov, "Restrictions on the energy and luminosity of $e^+e^-$ storage rings due to Bremstrahlung," Phys. Rev. Lett. **110**, 114801 (2013).
[64] T. Erber, "High-energy electromagnetic conversion processes in intense magnetic fields," Rev. Mod. Phys. **38**, 626 (1966).
[65] A. K. Harding and D. Lai, "Physics of strongly magnetized neutron stars," Rep. Prog. Phys. **69**, 2631 (2006).
[66] I. M. Ternov, "Synchrotron radiation," Phys. Usp. **38**, 409 (1995).
[67] J. M. Cole *et al.*, "Experimental evidence of radiation reaction in the collision of a high-intensity laser pulse with a laser-wakefield accelerated electron beam," Phys. Rev. X **8**, 011020 (2018).
[68] K. Poder *et al.*, "Experimental signatures of the quantum nature of radiation reaction in the field of an ultraintense laser," Phys. Rev. X **8**, 031004 (2018).
[69] M. K. Khokonov, "Cascade processes of energy loss by emission of hard phonons," J. Exp. Theor. Phys. **99**, 690 (2004).
[70] M. V. Bondarenco, "Multiphoton effects in coherent radiation spectra," Phys. Rev. D **90**, 013019 (2014).
[71] S. M. Ross, *Introduction to Probability Models*, 11th ed. (Elsevier, Amsterdam, 2014).
[72] B. Zhang, Z. M. Zhang, Z. G. Deng, W. Hong, J. Teng, S. K. He, W. M. Zhou, and Y. Q. Gu, "Effects of involved laser photons on radiation and electron–positron

pair production in one coherence interval in ultra intense lasers," Sci. Rep. **8**, 16862 (2018).
[73]B. Zhang, Z. M. Zhang, Z. G. Deng, J. Teng, S. K. He, W. Hong, W. M. Zhou, and Y. Q. Gu, "Quantum mechanisms of electron and positron acceleration through nonlinear compton scatterings and nonlinear Breit-Wheeler processes in coherent photon dominated regime," Sci. Rep. **9**, 18876 (2019).
[74]E. Esarey *et al.*, "Theory and group velocity of ultrashort, tightly focused laser pulses," J. Opt. Soc. Am. B **12**, 1695–1703 (1995).
[75]J. D. Jackson, *Classical Electrodynamics*, 3rd ed. (Wiley, New York, 1975).
[76]L. D. Landau and E. M. Lifshitz, *The Classical Theory of Fields*, 4th ed. (Elsevier, Singapore, 1975).